

Final report of K-112737 project

Summary

The goal of the proposed work is to better understand the major antiviral mechanisms/factors and the plant-virus interactions, which can lead to the plant recovery from virus infection. We have used several tools of molecular biology including transgenic plants, genome editing (CRISPR/CAS9), highthroughput technologies (such as deep sequencing, analysis of RNA targeting and gene expression at genome wide level, etc.), *in situ* hybridization and bioinformatics to explore in more details of the intimate interaction between the invading virus and the plant cell. We identified Argonaute (AGO) proteins involved in the antiviral plant response. We explored the effects of p19 virus encoded silencing suppressor protein on the small RNAs derived both from plant and virus and their target transcripts were also identified. Finally, we provided evidence that RNA silencing is not the reason for meristem exclusion in *Cymbidium ringspot virus* (CymRSV) infected *Nicotiana benthamiana* plants. Transcriptome analysis followed by *in situ* hybridization experiments shed light on the expressional changes in the shoot apical meristem (SAM) region upon virus infection. We observed a severe loss of meristem function in the SAM, which was accompanied by the downregulation of meristem-specific genes including *WUSCHEL* (*WUS*). Our findings suggest that the observed transcriptomal changes upon virus infection in the meristem and in the tissues close to meristem are the key factors in shoot necrosis and symptom recovery. More importantly we observed a significant down regulation in *GAPDH* level in tissues around the meristem, which likely explains the virus exclusion from the meristem. It is well known that the expression of GAPDH is essential for the replication of the invading virus and lacking GAPDH stops the virus replication and spread before it invades the meristem tissue. The activated RNA silencing although essential for recovery, but has no direct role in the viral meristem invasion.

Background

The outcome of virus infections of plants often resulted in symptom recovery, which is characterized by the emergence of new leaves showing attenuated or no symptoms. The symptom recovery often associated with exclusion of viruses from plant shoot apical meristems (SAM), however, the underlying mechanism of virus exclusion is very poorly understood. Recovery of plants from virus-induced symptoms is one of

the oldest mysteries in plant virology. The earliest report describing a plant defence mechanism has been published almost a hundred years ago, describing the plant recovery from virus infection. Tobacco plants infected with *Tobacco ringspot nepovirus* (ToRSV), which induced very strong necrotic symptoms in the initially infected leaves and later these plants recovered from the virus disease. The upper newly developed leaves looked healthy and were resistant to secondary infection of the same virus. At that time there was no explanation for this very interesting phenomenon. After the discovery of RNA silencing as a defence mechanism against invading molecular parasites, it was shown that RNA silencing plays a key role in the development of plant recovery from virus disease

RNA silencing is a conserved eukaryotic pathway involved in almost all cellular processes like development, stress responses and genome defence. RNA silencing relies on the 21–24 nt short interfering RNAs (siRNAs) or microRNAs (miRNAs) the hallmark molecules of silencing. These siRNAs have been shown to be mobile and to play an important part in the cell-to-cell and long-distance (systemic) spreading of silencing. Viruses can suppress RNA silencing in different ways from interfering with its initiation to causing an arrest in the assembly of a functional RNA Induced Silencing Complex (RISC). One of the best known VSR is the p19 protein of *Cymbidium ringspot virus* (CymRSV) identified previously in our laboratory, which inhibits silencing by binding the siRNAs in size-specific manner thereby inhibiting their incorporation into the RISC.

The essential role of RNA silencing in the recovery phenotype was demonstrated using mutant virus infection in which viral encoded silencing suppressor p19 protein was inactivated. In these reports it has been shown that the VSR inactivated virus initially caused severe symptoms, which gradually disappeared in the newly developed upper leaves and the virus RNA content of these leaves reduced below the detection level and showed resistance against to virus-containing homologous sequences. It assumed that the virus causing the initial symptoms had activated viral RNA silencing that inhibited the spread of virus infection into the upper leaves and caused them to be specifically immune to secondary infection of the same virus.

Plant recovery is often associated also with the exclusion of viruses from plant shoot apical meristems (SAM), which is one of the main plant meristems (shoot apical

meristem and the root apical meristem). The stem cells in these niches are maintained by a regulatory network. One of the main components of this network in the SAM is the homeodomain transcription factor WUSCHEL (WUS) and the CLAVATA (CLV) ligand-receptor system. *WUS* is expressed in the organizing centre, the middle of the central zone of the meristem and is required to induce and maintain the overlying stem cells in an undifferentiated state. Another homeodomain transcription factor that acts in parallel with WUS in maintaining the meristem is SHOOT MERISTEMLESS (STM). There are suggestions that the virus exclusion from the meristem has a role in the plant recovery and the meristem exclusion has been attributed to RNA silencing mechanisms.

Results

According to our work plan for the first year we generated of synthetic p19 expressing transgenic *N. benthamiana* plants. The rationale of this p19 expressing plant is to uncouple p19 effects of the virus infection on RNA silencing and host plant symptom development. To avoid the interference between the p19 transgene and the challenging virus (p19-deficient virus, Cym19stop), we made all possible silent nucleotide changes. In this way, we reduced the nucleotide sequence similarity between the transgene and the challenging virus to 68% while keeping the amino acid identity at 100%. These plants were named synthetic-p19 expressing plants (p19syn). The plant line 1-57 accumulating high levels of p19 were selected for further studies. The p19syn plants showed strong phenotype with elongated stem internodes and leaves distortion suggesting that the expressed p19 protein retained its suppressor activity, thus potentially compromising the endogenous silencing pathways. Importantly, this phenotype however was clearly different from that of virus infected stunted dwarf plant. We also tested the silencing suppressor activity of transgenically expressed p19 in a GFP transient assay. When GFP sense transgene was transiently expressed in wild-type plant leaves, the spontaneously triggered silencing almost completely diminished GFP expression at four dpi. In contrast, when GFP was expressed in p19syn plants its expression was still strong at four dpi as visualized under UV light. The lack of GFP silencing in p19syn plants confirmed the suppressor activity of the p19. Next we tested p19 suppressor activity in an authentic virus infection context: we challenged the p19syn plants by the infection with Cucumber mosaic virus and yellow satellite RNA (CMV-Y satRNA). CMV-Y-satRNA was

reported to induce bright yellow symptoms on *N. benthamiana* through targeting a gene involved in chlorophyll biosynthesis by Y-satRNA derived siRNAs. The CMV-Y-satRNA infected wt *N. benthamiana* plants developed the bright yellow symptoms while the infected p19syn plants failed to show the typical yellowing. All these data confirmed that the transgenically expressed synthetic p19 works as a silencing suppressor *in planta*. To explore the role of RNA silencing in the recovery phenomenon p19syn and wt *N. benthamiana* plants were infected with p19 deficient Cymbidium ringspot parental virus (Cym19Stop). As we expected from our previous studies after the initial strong viral symptoms on wt *N. benthamiana* plant recovered from virus infection and the newly developed leaves did not show viral symptoms. In contrast, the Cym19Stop infected p19syn plants were dwarf and the new leaves showed strong viral symptoms, however these viral symptoms were different from the phenotype of mock-inoculated p19syn plant.

It is generally assumed that virus encoded suppressors strongly interfere with the endogenous silencing pathway and are central players in the development of viral symptoms. However, this notion mostly comes from studies that used VSR-expressing transgenic plants without analysing the effect of the VSRS in an authentic virus infection background. To reinvestigate this dogma we set up an experiment in which we could compare p19 effects (vsiRNA and endogenous miRNA binding) with or without its parental virus infection background. Using wt and p19syn plants in combination with CymRSV and Cym19stop, we were able to analyze the effects of p19 provided “in trans” and “in cis” during the viral invasion of the plant. We have shown by sequencing the p19 bound small RNAs (sRNAs) that p19 can efficiently sequester endogenous small RNAs (sRNAs) in mock-inoculated p19syn plants while it does not bind these sRNAs upon Cym19stop infection. Also, the presence of p19 in virus infection did not alter the expression of miRNAs significantly. To better understand the biological relevance of vsiRNA-mediated endogenous sRNA binding and out-competition/release from p19 sequestration we analyzed the expression of known miRNA-target mRNA pairs. We compared RNAseq data obtained from mock-inoculated p19syn plant samples (when p19 binds to miRNAs) and from Cym19stop virus-infected p19syn plant samples (when p19 binds preferentially vsiRNAs while miRNAs are outcompeted/released). In the absence of the virus, p19 efficiently bound miRNA duplexes and this correlated with elevation of most of the miRNA-target mRNAs as the consequence of miRNA duplex sequestration by p19 and inability to

program miRISC for cleavage (p19syn compared to wt *N. benthamiana*). Upon Cym19stop virus infection however, the levels of most miRNA target RNAs were downregulated (compared to mock-infected p19syn) as the consequence of miRNA out-competition/release from p19. We went further and specifically looked to accumulation of trans-acting RNAs derived from TAS3 precursor, the target of miR390 in a Northern blot assay. In p19syn plants the level of miR390 was slightly elevated while the TAS3-derived D7 tasiRNA dropped below the detection level (compared to wt *N. benthamiana*). This was likely the consequence of the inhibition of the cleavage of TAS3 transcripts by p19-captured miR390. Indeed, miR390 is efficiently enriched in p19 IP (p19syn mock-infection). When p19syn plants were infected with Cym19stop virus, miR390 binding by p19 decreased and consequently the activity of miR390 was restored that lead to D7 tasiRNA accumulation (to a similar level as detected in wt *N. benthamiana*). Altogether our findings support the hypothesis that during virus infection p19 preferentially binds vsiRNAs while endogenous sRNAs are outcompeted/released from binding.

Importantly, these findings do not support the widely accepted assumption that viral symptoms are the direct consequence of the impact of VSRs on endogenous silencing pathways.

We also demonstrated that p19 preferentially sequesters positive:negative viral short interfering RNAs (vsiRNAs) pairs and that the binding by p19 is independent of vsiRNA sequence or the type of the 5'-end nucleotide. Finally using AGO1- and AGO2- immunoprecipitation experiments we observed that p19 specifically compromises vsiRNAs' loading into AGO1 but not AGO2. Since antiviral silencing is strongly inhibited by p19, this suggests that AGO1 is the main effector protein against CymRSV tombusvirus.

Regardless of the reason of how AGO1-loading is compromised by p19, it seems that AGO2 is not enough to fight off the virus and help the plant to recover in the absence of AGO1-loading/activity. It has been suggested previously that AGO2 but not AGO1 plays role in the antiviral response against tombusvirus infections, including Tomato bushy stunt virus (TBSV). We have done TBSV-VIGS (Virus Induced Gene Silencing) experiment, using p19 inactivated virus vector (TBSVp19stop), which carried Nb-PDS and Nb-AGO1 sequence. When NbAGO1 was silenced by VIGS the virus accumulated at higher level and plants have shown stronger phenotype. The obtained results further support the idea that AGO1 has a major role in antiviral

response against tombusvirus infection.

More details about our analysis and results are available on the link below:

<https://journals.plos.org/plospathogens/article?id=10.1371/journal.ppat.1005935>

Distinct Effects of p19 RNA Silencing Suppressor on Small RNA Mediated Pathways in Plants.

Kontra L, Csorba T, Tavazza M, Lucioli A, Tavazza R, Moxon S, Tisza V, Medzihradzky A, Turina M, Burgyán J. PLoS Pathog. 2016 Oct 6;12(10):e1005935. doi: 10.1371/journal.ppat.1005935. eCollection 2016. IF: 7,003

Since the role of AGO2 in tombusvirus infection was under debate we decided to further clarify the role of AGO2 in different plant virus interactions. We have set up the CRISPR/Cas system in *N. benthamiana* plants, to inactivate AGO2 important plant effector, which previously suggested that plays an important role in the antiviral silencing based plant response. However these studies predominantly used mutants of *Arabidopsis thaliana*, which is non a host for many economically important plant viruses including tombusviruses. Therefore we extended our study for the virological model plant, *N. benthamiana* and used the CRISPR/Cas9 technology to inactivate the AGO2 gene of *N. benthamiana*. The ago2 knock out plants exhibited different plant response against various viruses. AGO2 is a critical effector of the silencing based plants' immune responses against different plant viruses such as *Potato virus X* (PVX), *Turnip mosaic virus* (TuMV) and *Turnip crinkle virus* (TCV). In contrast, the lack of AGO2 does not significantly compromise the plant recovery of plant infected with the suppressor deficient mutants of tombusviruses, such as *Cymbidium ringspot virus* (CymRSV) and *Tomato bushy stunt virus* (TBSV). These findings further supported our previous results (Kontra et al., 2017. PLOS Pathogenes), that the main antiviral effector against tombusviruses is AGO1.

Detailed results are available on the link below:

<https://www.nature.com/articles/s41598-017-01050-6>

Ludman M, Burgyán J, Fátyol K. Crispr/ Cas9 Mediated Inactivation of Argonaute 2 Reveals its Differential Involvement in Antiviral Responses. Sci Rep. 2017 Apr 21;7(1):1010.

Plant recovery, often associated with exclusion of viruses from plant shoot apical meristems (SAM), as demonstrated in previous reports. In addition, it was suggested that the meristem exclusion has been attributed to RNA silencing mechanisms. However, our observations contradict this widely assumed explanation. We have shown previously in several studies that CymRSV, which used in our study expresses the strong RNA silencing suppressor p19 protein. It is also well known that CymRSV causes a fast tip necrosis of the infected plants. However, our *in situ* studies also shown that CymRSV is not able to invade the meristem of infected plants, but causes tip necrosis. These results does not support the previous explanation that the meristem exclusion has been attributed to RNA silencing since CymRSV's p19 protein efficiently inhibits RNA silencing during the virus invasion.

To further test whether the antiviral silencing has a key role in the meristem invasion, we infected *N. benthamiana* plants with CymRSV expressing the p19 strong RNA silencing suppressor protein and performed *in situ* hybridization on infected *N. benthamiana* shoots following the protocol previously described by our group. Our *in situ* analysis showed that both the wt and the p19 deficient viruses had been excluded from SAM (Fig. 1) demonstrating that the inactivation of the antiviral silencing response by the p19 VSR is not enough to invade the SAM by the replicating viruses. Since the CymRSV-induced shoot necrosis is quite fast, we also used the Cym19stop mutant virus that cannot spread further than a few cell layers from the veins and a transgenic *N. benthamiana* plant expressing a synthetic version of p19 VSR of CymRSV (p19syn plant). The p19 mutant virus can spread in these plants similarly to the CymRSV in wild type plants, although the process is a bit slower due to the lower amount of p19. In contrary to our expectations (based on previous studies with other viruses), we could not detect the CymRSV in any of the shoot meristems of virus-infected plants, not even in the presence of enhanced amount of p19 (P19syn plant infected with CymRSV) and at low temperature, which also inhibits RNA silencing (Fig. 1). This indicates that meristem invasion is not the consequence of the suppression of RNA silencing by the p19 VSR and low temperature. These results indicate that RNA silencing is not the key factor in meristem invasion. On the other hand, the suppression of virus-induced antiviral silencing is crucial for the high accumulation of viral RNAs in plant shoot (excluding the meristem) and for the development of fast shoot apical necrosis, as it was previously demonstrated.

To have a better view of the spatiotemporal progression of infection and the transcriptional changes in virus-infected plant shoot apices, we performed a series of *in situ* hybridizations (Fig. 2). This experiment showed that after 3 dpi the virus is already present in the shoot, but the endogenous transcription of the housekeeping *GAPDH* and the pathogen-related *PRQ* (a.k.a. *PR3*) are unchanged. In contrast, after 4 dpi, in the virus-invaded plant tissues close to the SAM, the *GAPDH* level is undetectable, while the pathogenesis-related *PRQ* is greatly induced. It is worth noting that *GAPDH* is essential for the replication of the invading virus and lacking *GAPDH* stops the virus replication and spread before it invades the meristem tissue. Although the wt virus was clearly excluded from the SAM, it was able to induce shoot necrosis of the plant. More importantly, the virus infection specifically inhibited the expression of SAM specific genes such as *WUS*, the central player of the meristem-specific regulatory network (Fig. 3a). These results strongly suggest that the loss of *WUS* (and other meristem-specific genes) function results in meristem collapse and the high accumulation of virus close to the meristem lead to tip necrosis. It is worthy to note that the meristem collapse alone does not induce shoot necroses as was observed using *wus-1* loss of function mutant. The *WUSCHEL* gene is required for shoot and floral meristem integrity in *Arabidopsis*.

The above *in situ* data suggests that there is a sharp change in the expression patterns from 3 dpi to 4 dpi. Thus, to capture these gene expression changes caused by the advancing virus infection, we collected meristem tissue samples from 4 dpi mock and CymRSV infected plants in four biological replicates (3×15 meristem for each replicate) for transcriptome analysis. It is important to note that these samples contained not only meristem cell but also tissues close to the meristem as indicated in Fig. 2.

Analysing the obtained high-throughput sequencing data in details (See Fig. S1–5) we can conclude that the upregulated genes are mainly related to cell defence (plasma membrane located receptor kinases, hypersensitive response, salicylic acid and ethylene signalling), while the downregulated genes are related to DNA replication and organization, shoot meristem development, programmed cell death, and plasmodesmata function.

Although many transcripts were upregulated upon CymRSV infection, most of the already known meristem-regulating genes were downregulated in our dataset (Fig. S3). To explore how well the transcriptome analysis captured the changes in the meristem (Fig. S2) and to distinguish these changes from those in the infected tissue part, we performed *in situ* hybridization with a few selected genes (Fig. 3). According to the RNA-seq data, in this experiment, *WUS*, which is essential to maintain the meristem, was not detectable in the organizing centre (OC) after 4 dpi. The level of *SHOOT MERISTEMLESS (STM)* is also decreasing, indicating that the meristem function is disturbed. As even the stress related *PRQ* was upregulated only in the infected tissues and not detectable in the meristem (Fig. 2), we were wondering if we find any genes upregulated in the meristem. For this purpose, we selected a few genes showing upregulation in our RNA-seq data and performed *in situ* hybridizations with them. This showed that most of the upregulated genes expressed at a higher level only in the infected tissue (Fig. S6). However, *DMR6*, which was strongly expressed in the peripheral zone of the meristem was upregulated only in the uninfected meristem cells (Fig. 3C). *H2* was also strongly downregulated in the infected shoots (Fig. 3C). These data suggest that the meristem is not functional anymore and that these changes are likely programmed as a consequence of the accumulated virus in the tissues around meristem.

We wondered if the downregulation of *WUS* has any connection to the previously reported „shut-off” phenomenon when the downregulation of host gene expression is associated with the virus replication. To test this, we extended our experiments with *Tobacco vein clearing virus (TVCV; former crTMV)* and *Cucumber mosaic virus (CMV)* infected samples (Fig. 4). It is well known that TVCV causes „shut-off” and similar symptoms (shoot necrosis) as the CymRSV infection. We got similar results as with CymRSV (Fig. 4) except the expression of *WUS*, which was unchanged compared to mock even after 6 dpi. CMV infection does not cause „shut-off” and results in weak symptoms. Importantly, in these samples, the *WUS* expression stays on, similarly to the TVCV infection, and as expected, the *GAPDH*, *H2*, and *STM* expressions were also unchanged (Fig. S7 and S8). Interestingly, the *PRQ* expression is upregulated at 4 dpi but then decreases again. Taking together, these results show that the downregulation of *WUS* is specific to CymRSV infection and it is not the consequence of the activated shut-off. Moreover, there is no direct connection

between the downregulation of *WUS* and the shoot necrosis in general, since the TVCV necrotized the plant shoot while CMV didn't.

Our results clearly demonstrated that in a compatible interaction between a virus and its host plant, the virus infection causes drastic alterations in the plant transcriptome leading to symptom development. In many cases, symptom attenuation can be seen in the upper part of the plant, called recovery. The capability for recovery depends on the host plant species/variety–virus interaction and influenced by environmental factors, such as temperature. Recovery is also linked to gene silencing and its dependence on temperature. In these experiments, the infected plants were grown at various temperatures after infection which resulted in that at 27°C the virus could not invade the whole leaf blade or spread close to the meristem leading to recovering from the infection. Here we tested whether the plants can recover at 27°C after they developed shoot necrosis at 21°C. We found that most of the infected plants grown 4 dpi at 21°C and then 5 days at 27°C could recover but only from the axillary buds (Fig. S9) showing that the reprogramming of the transcriptome is not reversible by the temperature, and leads to the loss of SAM function. Our data suggest that the loss of meristem function is not because of lost *WUS* expression but a result of a reprogrammed hormonal network.

It is worth noting that the expression of *SIZ1* homologues are upregulated and they are in the significantly enriched GO category called 'ubiquitin-like protein transferase activity' (Fig. S10). The *SIZ1* gene is a regulator of SA signalling, immunity, and shoot development making it a good candidate as a silencing-independent factor of virus-induced meristem shut-down. Recently, an autophagy-related gene, Beclin1 was shown to be induced by TuMV infection and restrict viral replication in *N. benthamiana* plants by binding to the viral replicase protein. Beclin1 was also induced in our samples, along with other autophagy-related genes, which suggests that this mechanism of viral restriction is not a TuMV-specific response and that virus-induced autophagy is a common response to virus infection. Taken together our in situ and transcriptome analysis highlight the high variability of plant strategies to counterreact the invading viral pathogens. The manuscript prepared from these results was submitted for publication and it is under review. The manuscript is available upon request.

Related to our main study we were also involved in a collaborative work discovering the cooperation of RNA silencing and nonstop decay, which have key role in transcription regulation and plant mRNA quality control systems. We characterized the mechanism of nonstop decay (NSD) system in *Nicotiana benthamiana* model plant. We have shown that plant NSD efficiently degrades nonstop mRNAs, which can be generated by premature polyadenylation, and stop codon-less transcripts, which are produced by endonucleolytic cleavage. We demonstrated that in plants, like in animals, Pelota, Hbs1 and SKI2 proteins are required for NSD, supporting that NSD is an ancient and conserved eukaryotic quality control system. Relevantly, we found that NSD and RNA silencing systems cooperate in plants.

The obtained results have been published in *Nucleic Acids Research*, 2018, Vol. 46, 4632–4648.

<https://academic.oup.com/nar/article/46/9/4632/4972878>

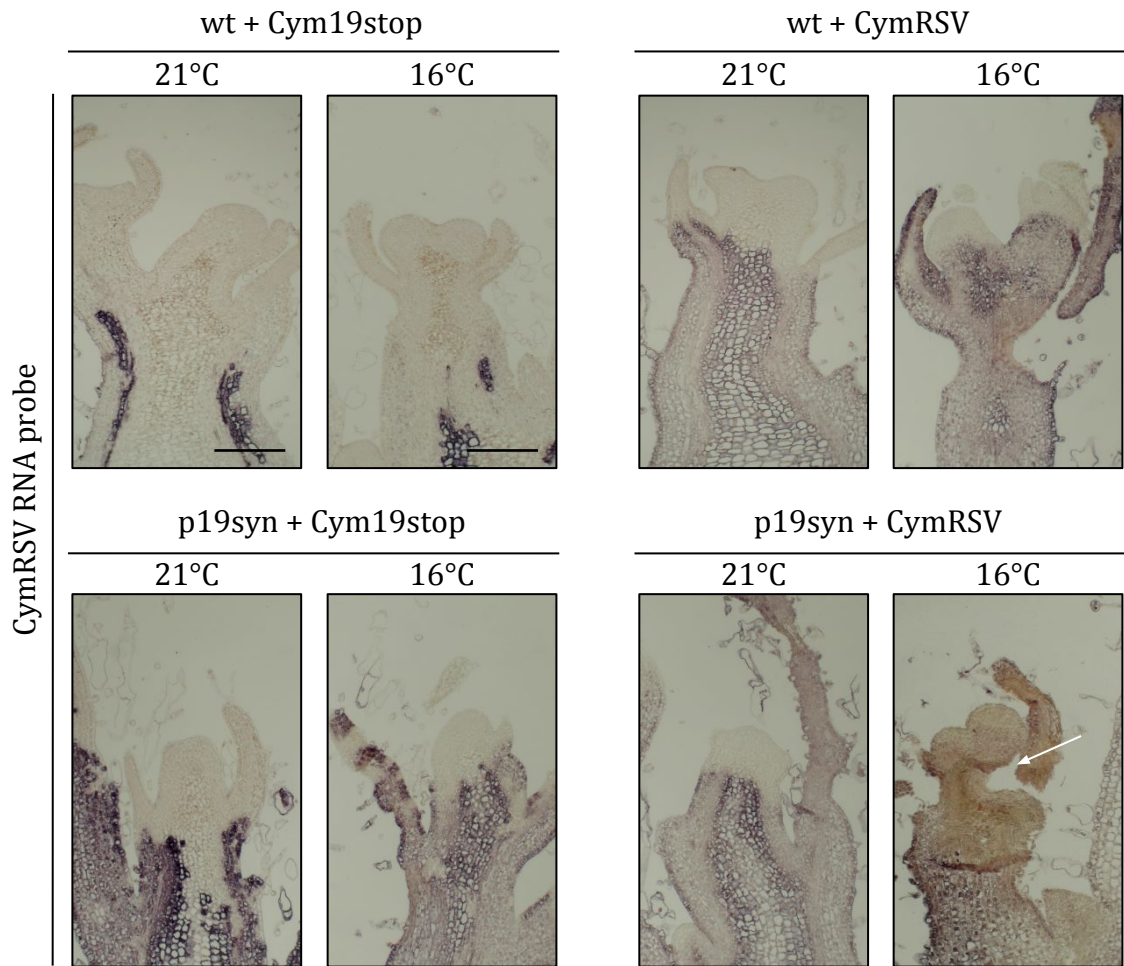


Fig. 1 Detection of CymRSV in the SAM by *in situ* hybridization.

Representative pictures of three *in situ* hybridizations of consecutive longitudinal sections of infected meristems ($n = 3-10$) hybridized with CymRSV-specific probes. Wild type *N. benthamiana* and transgenic plants expressing the p19 VSR of CymRSV (p19syn) were infected with wt CymRSV or the VSR mutant Cym19stop as indicated. Plants were grown at 21°C for 5 days or at 16°C for 9 days after inoculation. Arrow indicates necrotic tissue. Bars = 200 μm .

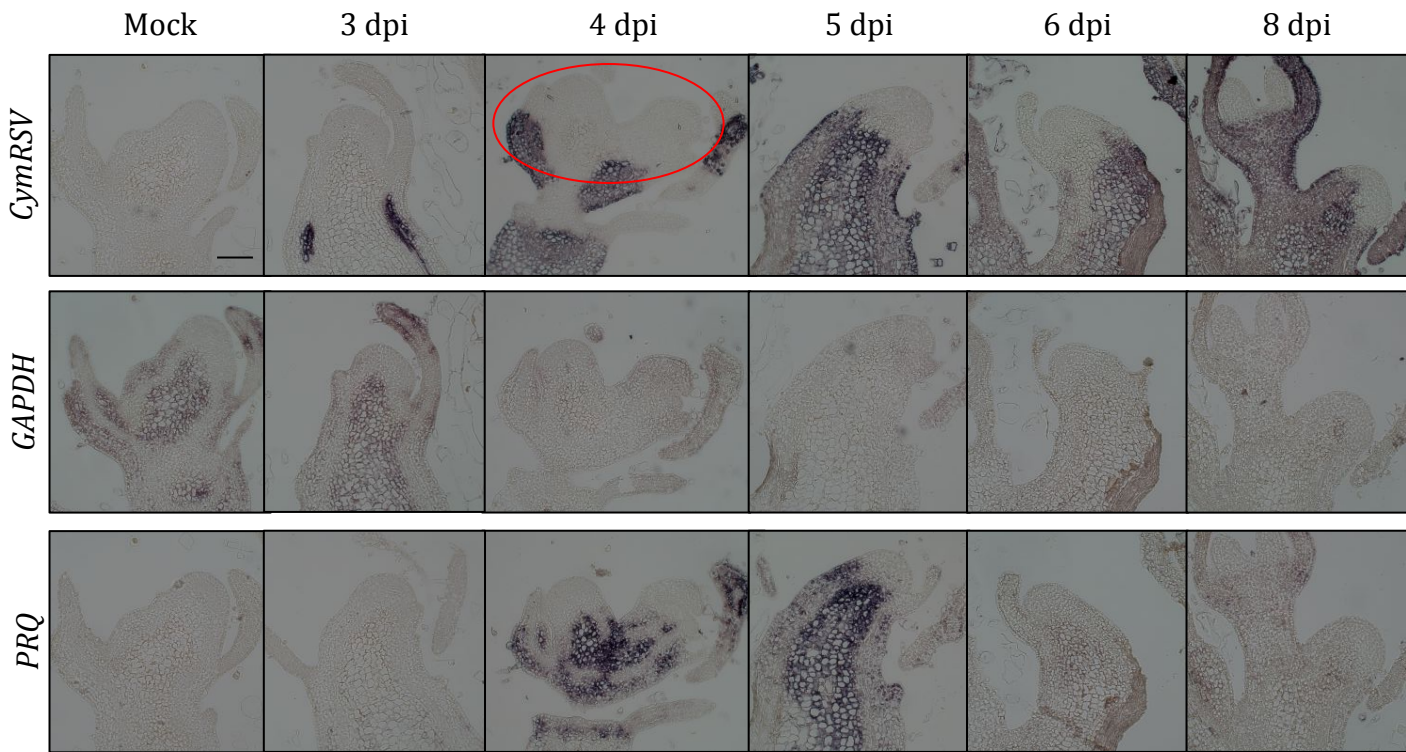


Fig. 2 Monitoring the movement of CymRSV in shoot apices in time.

In situ hybridization of longitudinal sections of mock-treated or CymRSV-infected SAMs 3 to 8 dpi, as indicated. Sections were hybridized with CymRSV- or gene-specific probes to detect *GLYCERALDEHYDE 3-PHOSPHATE DEHYDROGENASE A subunit 2 (GAPDH)*, *PATHOGENESIS-RELATED PROTEIN Q (PRQ)*. The red circle indicates the tissue collected for the RNA-seq experiments. Bar = 100 μ m.

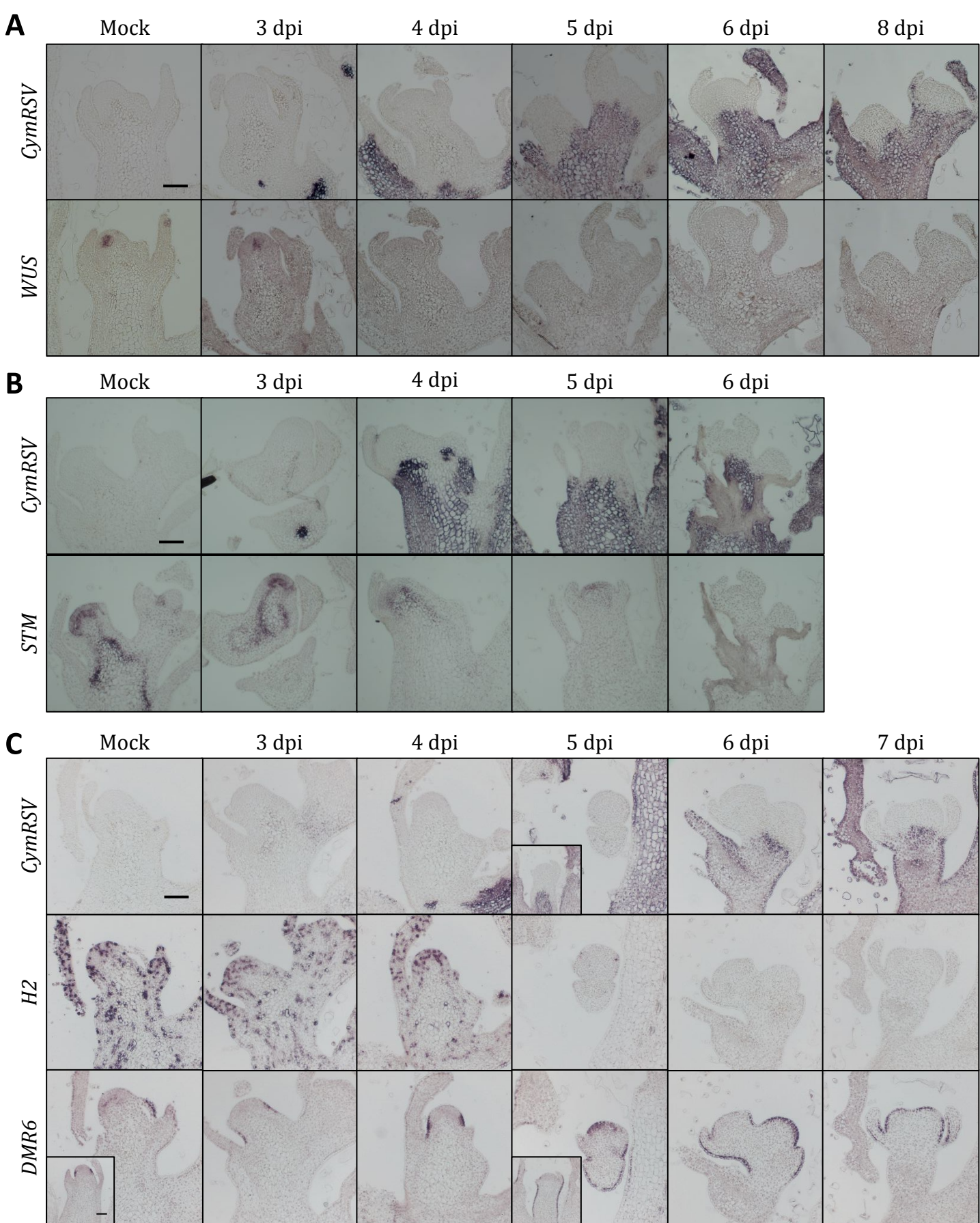


Fig. 3 Expression pattern of selected genes in *CymRSV*-infected shoot apices.

In situ hybridization of longitudinal sections of mock and *CymRSV*-infected plants hybridized with *CymRSV*- or gene-specific probes as indicated on the left side: **(A)** *WUSCHEL* (*WUS*), **(B)** *SHOOT MERISTEMLESS* (*STM*), **(C)** *HISTONE 2* (*H2*) and *DOWNY MILDEW RESISTANT 6* (*DMR6*). Note that meristems in **(C)** are from a different infection and embedding that can cause different timing in the expression changes. Bars = 100 μ m.

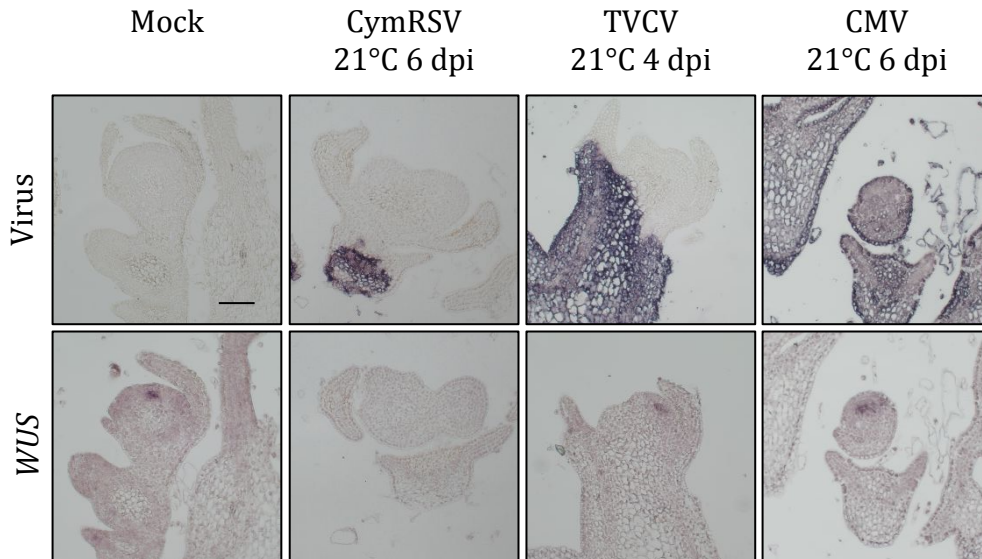
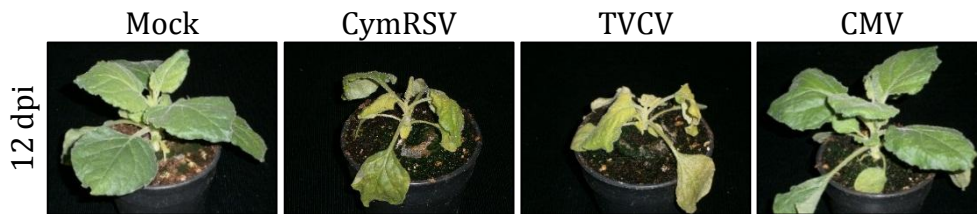
A**B**

Fig. 4 *WUS* expression and viral symptoms of plants infected with three different viruses.

(A) *In situ* hybridization of consecutive longitudinal sections of mock, CymRSV-, *Turnip vein-clearing virus* (TVCV), and *Cucumber mosaic virus* (CMV) infected SAMs hybridized with probes to detect the virus or *WUSCHEL* (*WUS*). Bar = 100 μ m. (B) Symptoms of mock, CymRSV-, TVCV-, or CMV-infected *N. benthamiana* plants 12 days after infection.

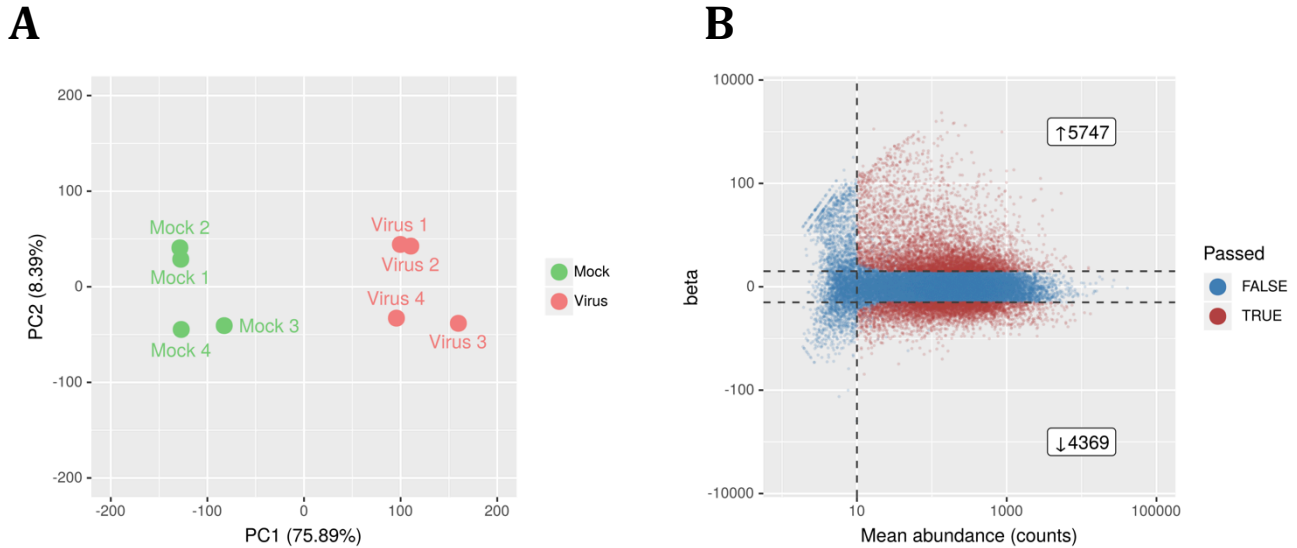


Fig. S1 Exploratory analysis of the RNA-seq data.

(A) Principal component analysis of the log₂-transformed, normalized transcript expressions (TPM) in the samples. We prepared four biological replicates per treatment. The first component explains more than two-thirds of the variances in the expression values and separates the mock and the virus-infected samples. **(B)** MA-plot showing the biased estimator of the fold-changes (the beta coefficient in the sleuth model) in the transcript expressions as a function of the mean transcript abundance (counts). The values shown in the axes are the exponentials of the original log-transformed values on a log₁₀ scale. The positive beta values represent increased, while the negative values represent decreased transcript expression in the virus-infected samples. For the differential expression analysis, the *P*-values were calculated using the Wald test and corrected for multiple testing to get the *Q*-values according to the Benjamini-Hochberg method at a false discovery rate of 1%. We considered a transcript differentially expressed if its mean abundance across the samples was at least 10 (vertical dashed line), the absolute value of its beta was at least 2 (horizontal dashed line), and its *Q*-value was less than 0.01. The red dots mark the transcripts that passed these filters. The numbers after the up- and the downward arrow denote the number of the up- and the downregulated transcripts, respectively.

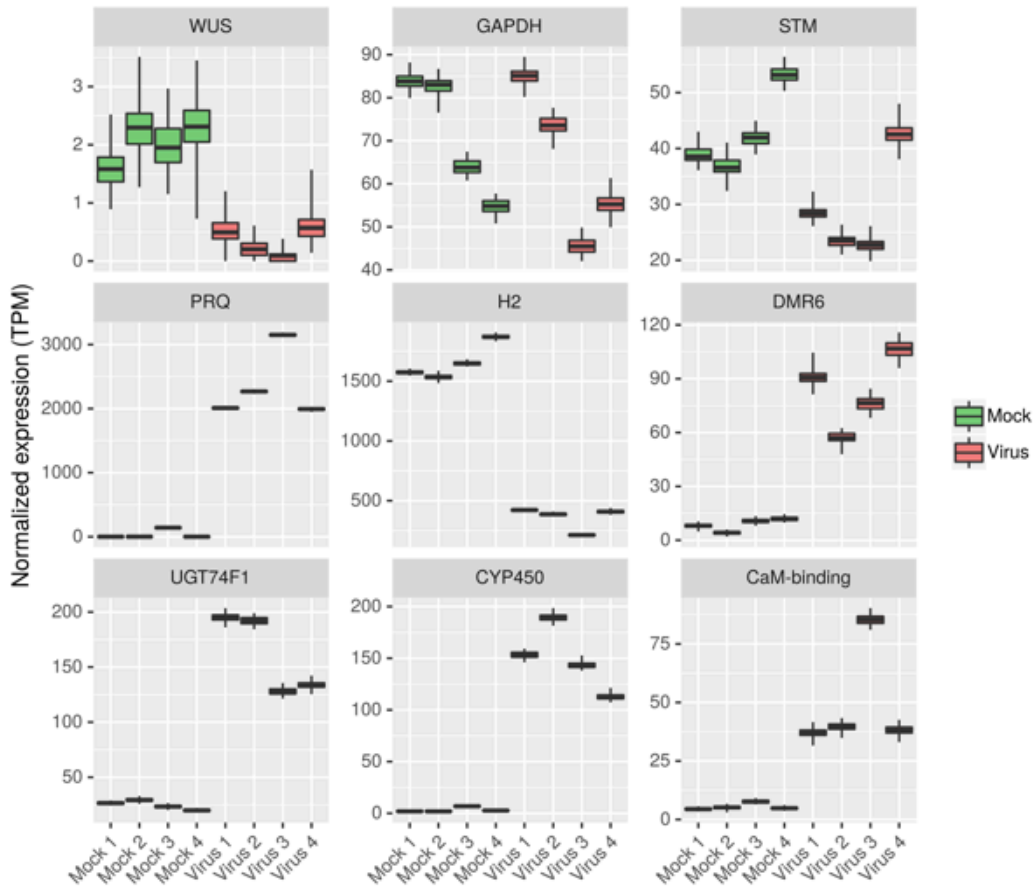


Fig. S2 Expression of selected genes that were analysed by *in situ* hybridization experiments.

The normalised expression values (transcript per million, TPM) of the indicated genes were estimated by kallisto (Pimentel *et al.*, 2017). The boxplots represent the summary of the bootstrap analysis which estimates the technical variances in a sample. Four biological replicates were prepared (Mock 1–4, Virus 1–4). The *WUSCHEL* (*WUS*) and the *SHOOT MERISTEMLESS* (*STM*) gene strictly expresses in the meristem, while the *GLYCERALDEHYDE-PHOSPHATE DEHYDROGENASE* (*GAPDH*) is an enzyme that is required for virus replication. The *PATHOGENESIS-RELATED Q* (*PRQ*) is a well-known stress-induced marker gene. *HISTONE 2* (*H2*), *DOWNY MILDEW RESISTANT 6* (*DMR6*) is a salicylic acid 5-hydroxylase, *UDP-GLYCOSYLTRANSFERASE 74 F1* (*UGT74F1*) transfers UDP:glucose to salicylic acid, *CYTOCHROME P450* (*CYP450*) is a hydroxylase involved in the metabolism of many bioactive compounds, including hormones, while *CALMODULIN-BINDING PROTEIN* (CaM-binding) is a component of many stress-related signalling pathways.

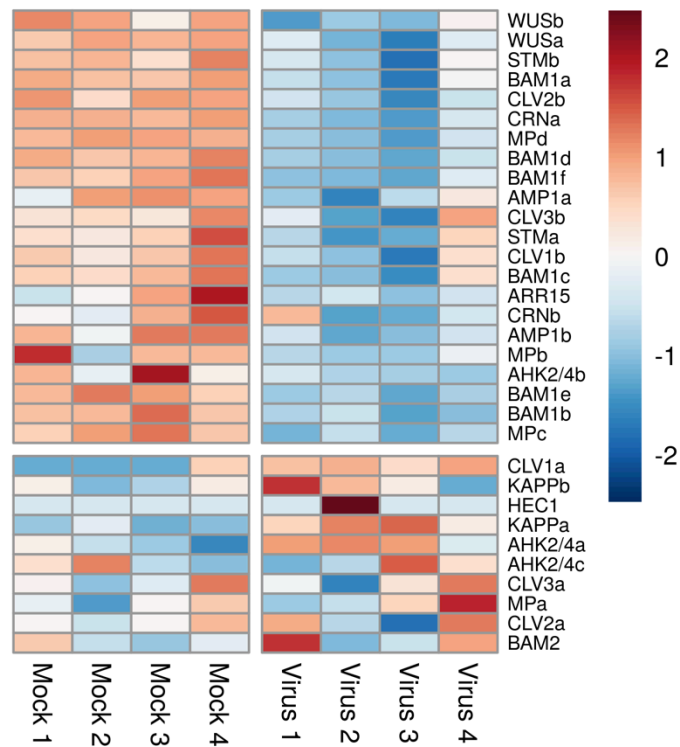
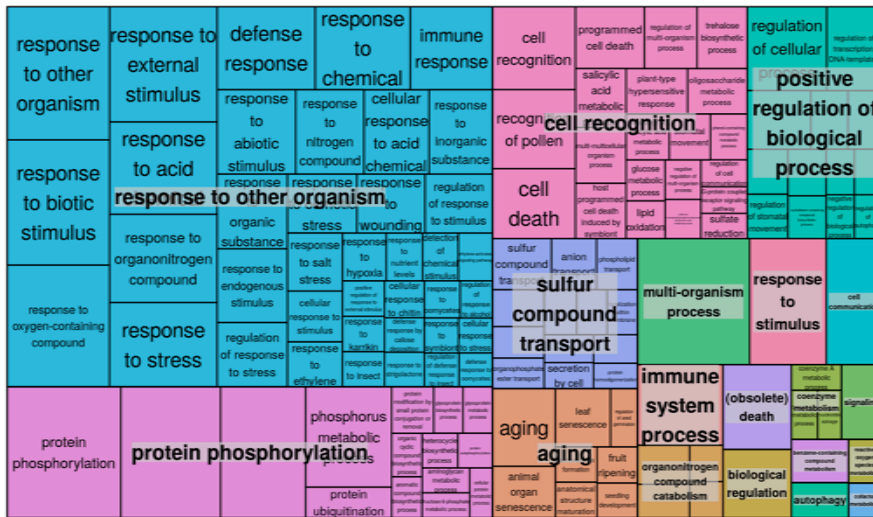


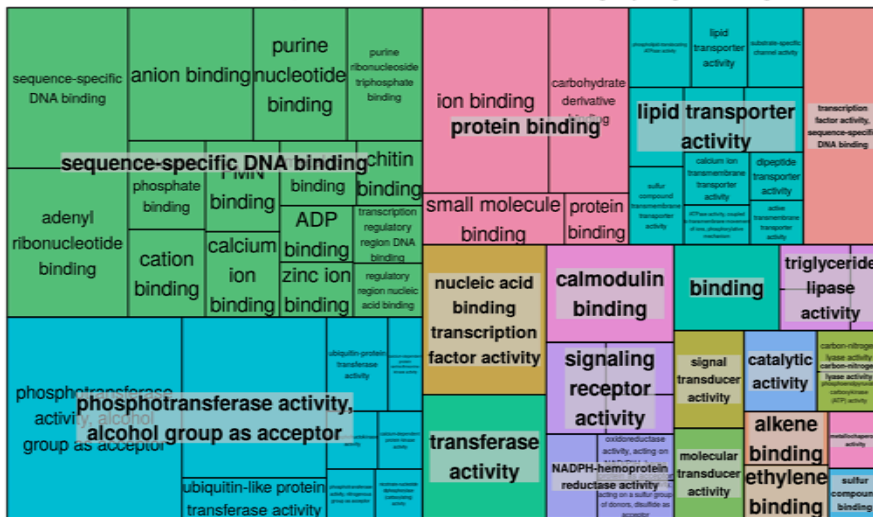
Fig. S3 Expression of meristem-specific genes.

The normalised expression values (transcript per million, TPM) of the indicated genes were estimated by kallisto (Pimentel *et al.*, 2017), log₂-transformed and z-scores were calculated. The z-scores show how many standard deviations the given value is above (red) or below (blue) from the mean (white) of all the values in the row. We show the values of the four biological replicates (Mock 1–4, Virus 1–4).

Enriched GO terms (Biological Process) among upregulated genes



Enriched GO terms (Molecular Function) among upregulated genes



Enriched GO terms (Cellular Component) among upregulated genes

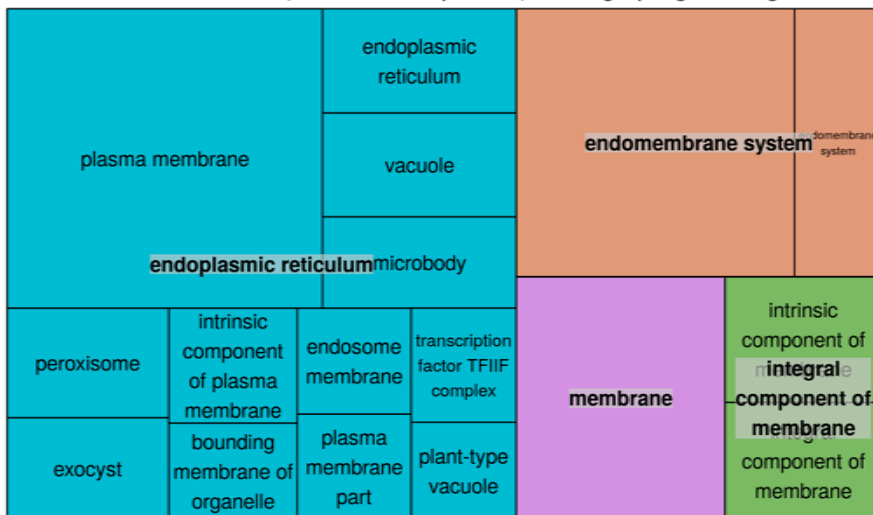
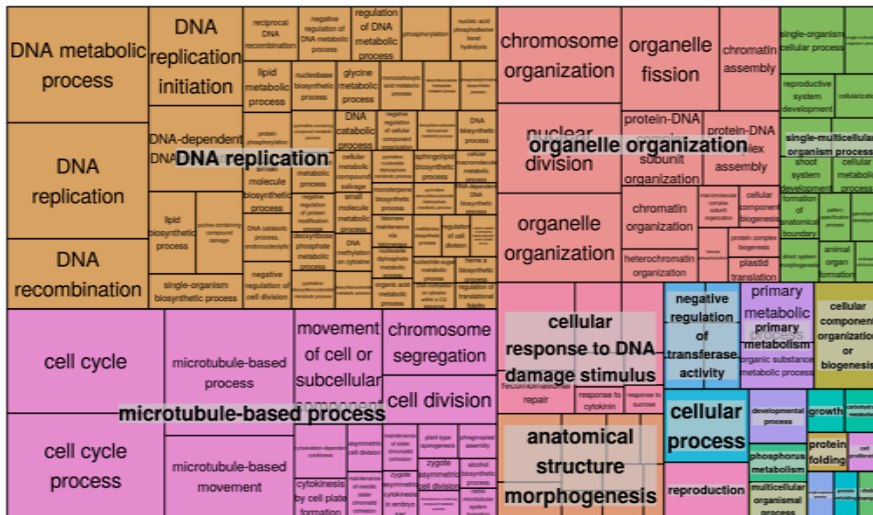


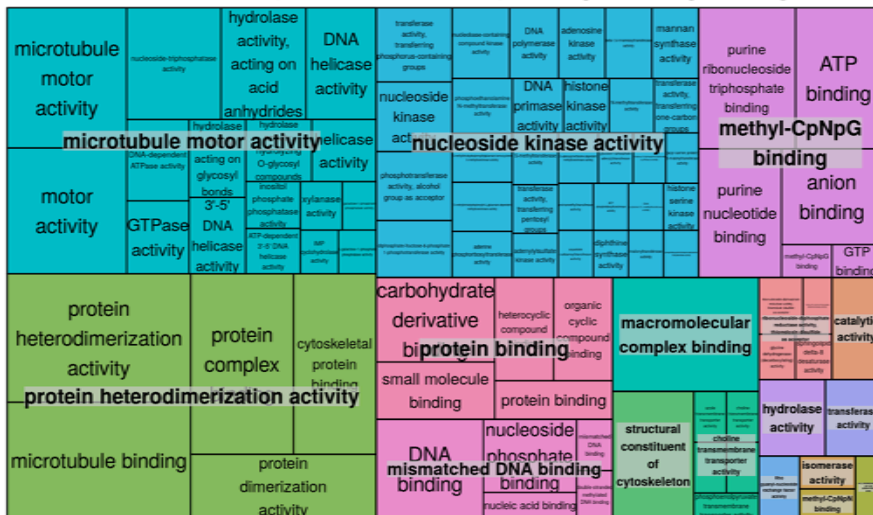
Fig. S4 Gene Ontology (GO)-term enrichment analysis of the upregulated genes.

The differential expression analysis was performed with sleuth (Pimentel et al, 2017). For the criteria considering a gene as differentially expressed see Fig. S2. We performed the GO-term enrichment analysis using PlantRegMap (Jin et al., 2017) and REVIGO (Supek et al., 2011).

Enriched GO terms (Biological Process) among downregulated genes



Enriched GO terms (Molecular Function) among downregulated genes



Enriched GO terms (Cellular Component) among downregulated genes

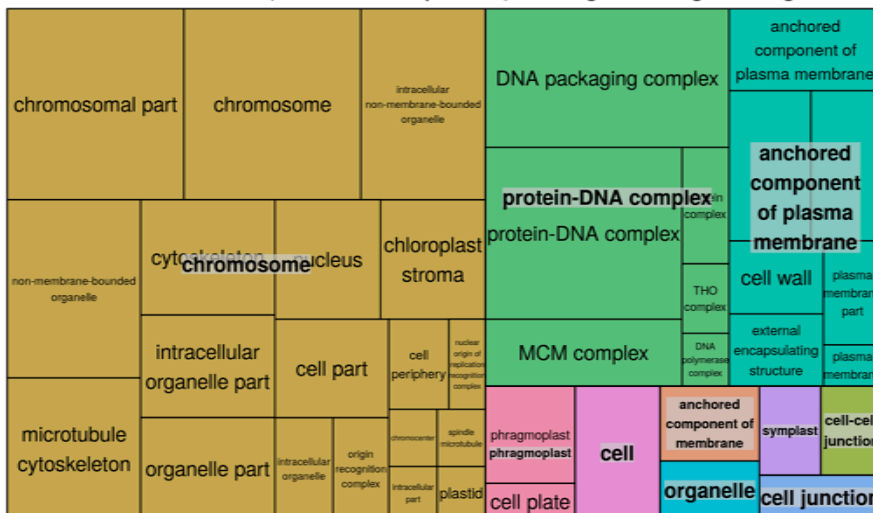


Fig. S5 Gene Ontology (GO)-term enrichment analysis of the downregulated genes. The differential expression analysis was performed with sleuth (Pimentel et al, 2017). For the criteria considering a gene as differentially expressed see Fig. S2. We performed the GO-term enrichment analysis using PlantRegMap (Jin *et al.*, 2017) and REVIGO (Supek *et al.*, 2011).

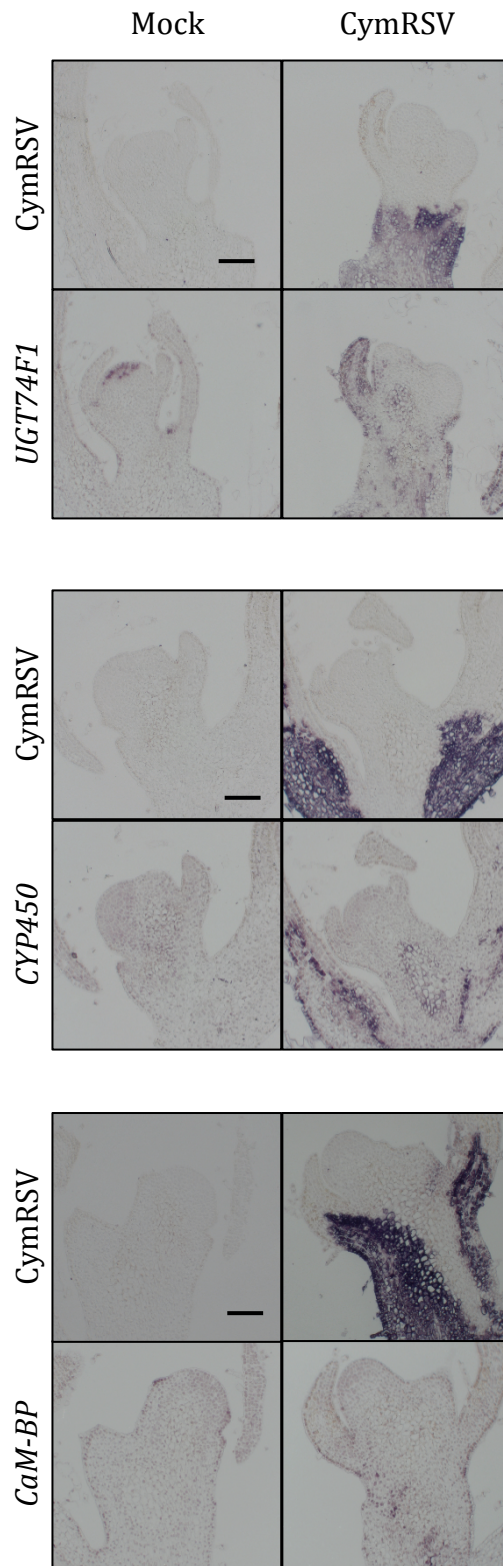


Fig. S6 Expression pattern of selected genes in CymRSV-infected shoot apices.

In situ hybridization of longitudinal sections of shoot apices of mock and CymRSV-infected plants 4 or 5 dpi, hybridized with CymRSV- or gene-specific probes as indicated: *UDP-GLYCOSYLTRANSFERASE 74 F1* (*UGT74F1*), *CYTOCHROME P450 SUPERFAMILY PROTEIN* (*CYP450*), or Calmodulin-binding (*CaM-BP*). Bars = 100 μ m.

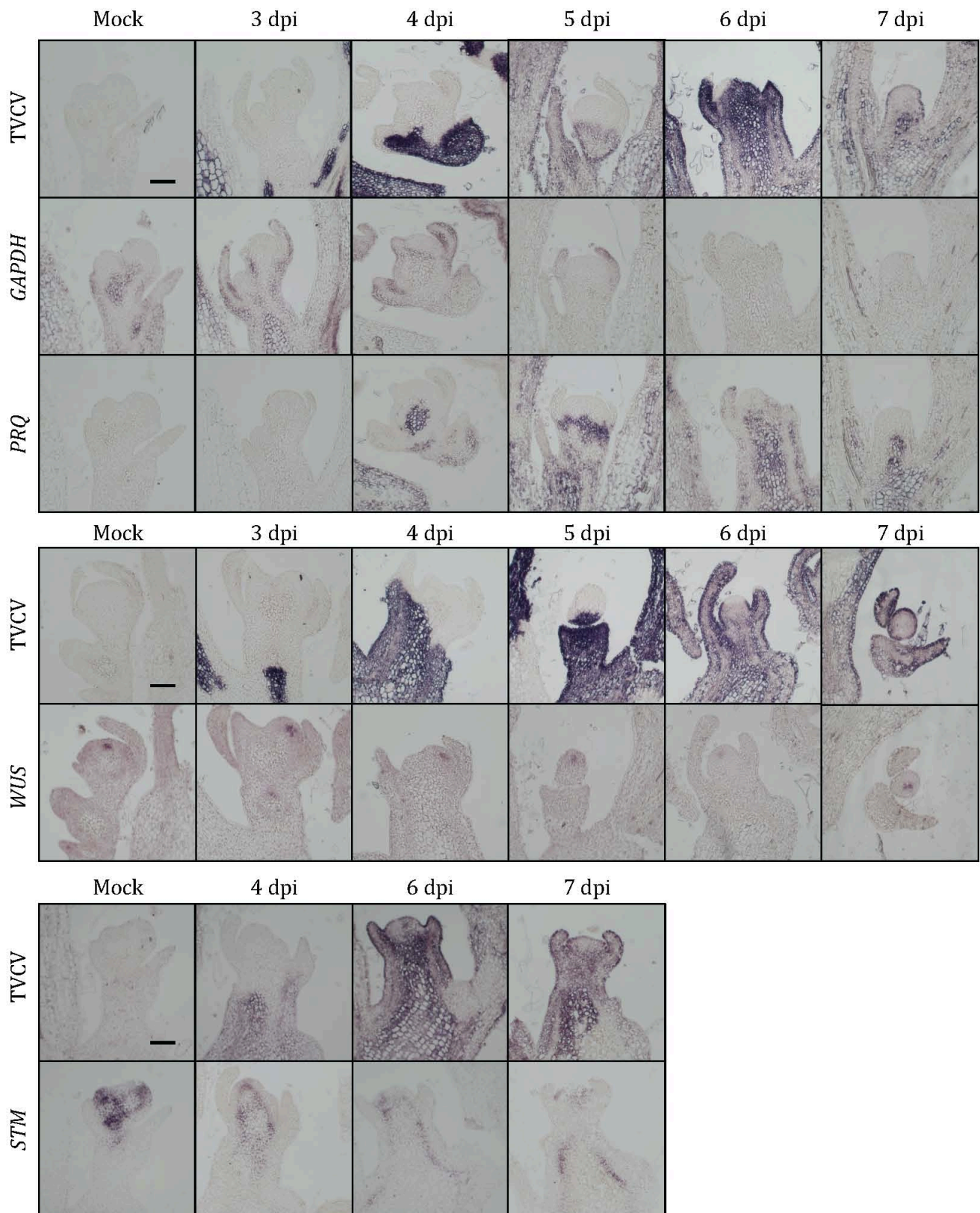
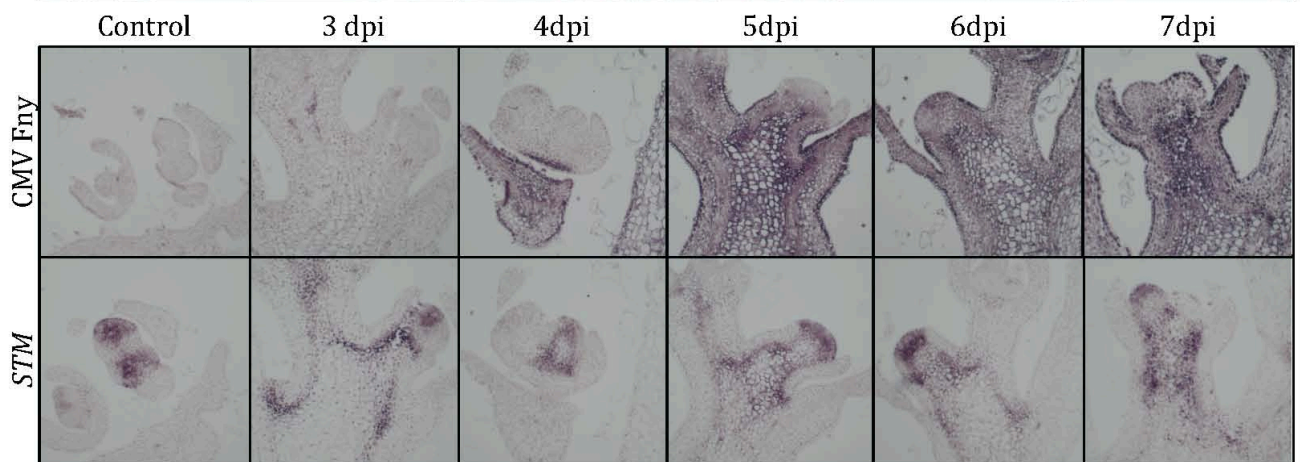
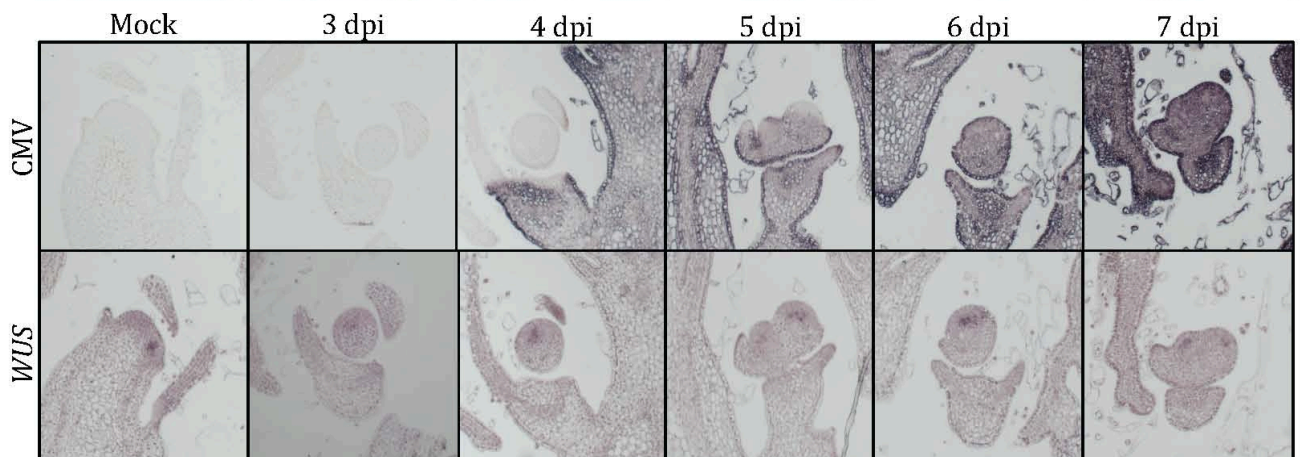
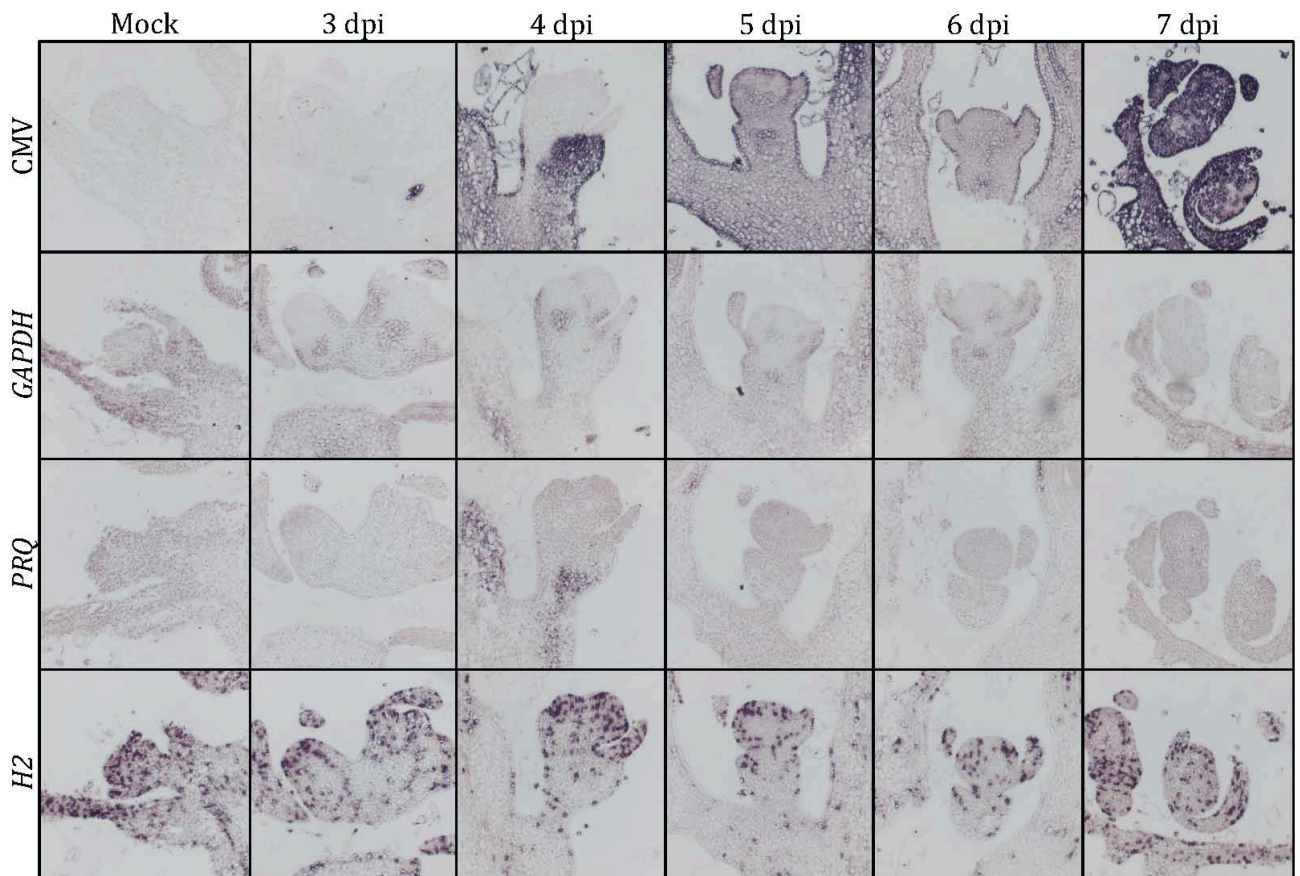


Fig. S7 *In situ* hybridization of *Turnip vein-clearing virus* (TVCV)-infected shoot apices.

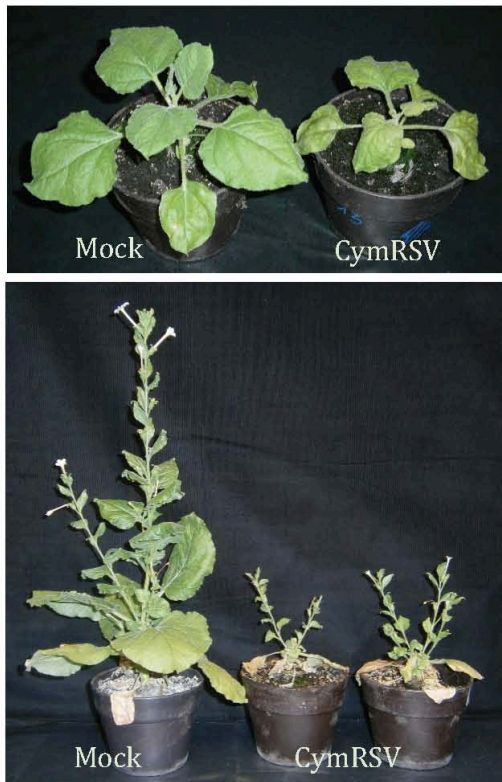
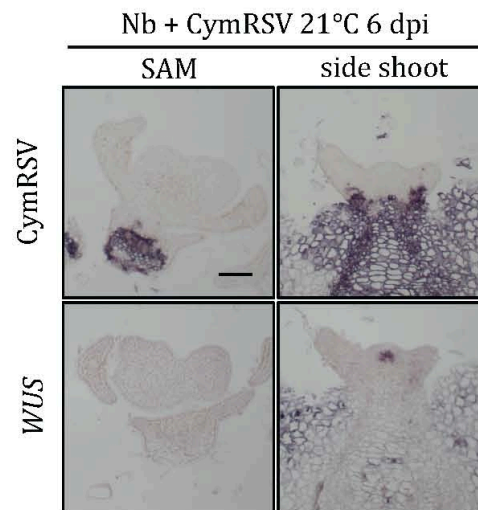
In situ hybridization of longitudinal sections of mock and TVCV-infected plants 4 or 5 dpi hybridized with a virus- or gene-specific probes as indicated: *GLYCERALDEHYDE 3-PHOSPHATE DEHYDROGENASE A SUBUNIT 2* (GAPDH), *PATHOGENESIS-RELATED PROTEIN Q* (PRQ), *WUSCHEL* (WUS), *SHOOT MERISTEMLESS* (STM). Bars = 100 μ m.



See figure legend next page.

Fig. S8 *In situ* hybridization of *Cucumber mosaic virus* (CMV)-infected shoot apices.

In situ hybridization of longitudinal sections of mock and CMV-infected plants hybridized with a virus- or gene-specific probes as indicated on the left side: *GLYCERALDEHYDE 3-PHOSPHATE DEHYDROGENASE A SUBUNIT 2* (*GAPDH*), *PATHOGENESIS-RELATED PROTEIN Q* (*PRQ*), *HISTONE 2* (*H2*), *WUSCHEL* (*WUS*), *SHOOT MERISTEMLESS* (*STM*). Bars = 100 μ m.

A**B****Fig. S9 Recovery from side shoots.**

(A) Symptoms of mock and CymRSV-infected *N. benthamiana* plants grown at 21°C 4–8 days after infection, then transferred to 27°C for 3 weeks. Symptoms of a representative mock and CymRSV-infected plants grown at 21°C one week after infection (upper picture) and at 27°C four weeks after infection (lower picture). (B) *In situ* hybridization of consecutive longitudinal sections of CymRSV-infected SAM and side shoot from plants grown at 21°C, 6 dpi. Sections were hybridized with CymRSV or *WUSCHEL* probes as indicated. Bar = 100 μ m.

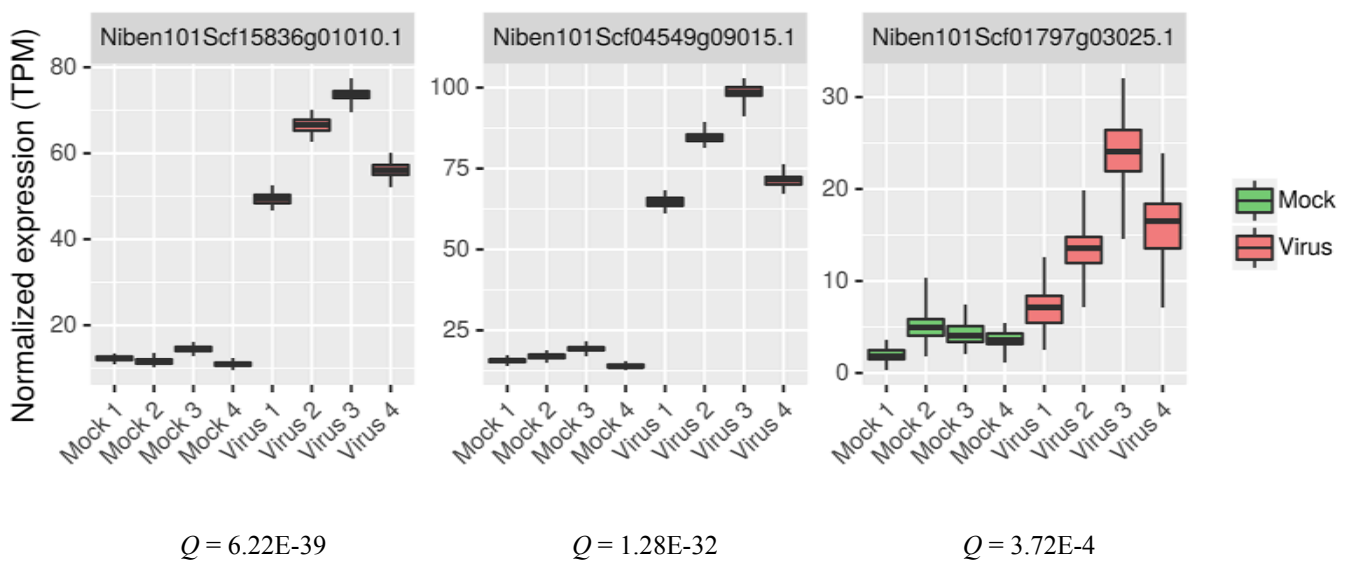


Fig. S10 Expression of the significantly upregulated *SIZ1* homologue genes in the SAM region.

The normalised expression values (transcript per million, TPM) of the indicated genes were estimated by kallisto (Pimentel *et al.*, 2017). The boxplots represent the summary of the bootstrap analysis which estimates the technical variances in a sample. Four biological replicates were prepared (Mock 1–4, Virus 1–4). For criteria of the significantly changed expressions see legend of Fig. S2.